Bipedal model experimentally adjusted to simulate human walking forces in vertical direction

Vega D. [1], Magluta C.[1], Roitman N.[1]

[1]*Dept. of Civil Engineering, Federal University of Rio de Janeiro*
Centro de Tecnologia, Bloco I 216, Ilha do Fundão, 21941-9726, Rio de Janeiro/RJ, Brazil
dianelys@coc.ufrj.br, magluta@coc.ufrj.br, roitman@coc.ufrj.br

Abstract. In this study, a damped bipedal model with compliant legs is adopted from the literature to represent a walking pedestrian. Forty-five volunteers are recruited to participate in an experimental program to walk on a rigid surface covered by force plates. The walking forces and accelerations at the pedestrians' center of mass are recorded in the experimental campaign. The bipedal model parameters are estimated by adjusting the numerical and experimental vertical ground reaction forces (GRFs). Monte Carlo simulations are performed within wide ranges of input parameters and initial conditions to obtain the best possible matches between the model predictions and experimentally measured data. It is found that the bipedal model can reproduce stable gaits and typical M-shape GRF profiles for step frequencies in the range of 1,42-2,42 Hz. The best correlations are found at slow and normal walking speeds. Moreover, empirical values for pendulum length, attack angle, leg stiffness and leg damping are proposed.

Keywords: Bipedal model, Human-induced loads, Experimental calibration

1 Introduction

The simulation of loads induced by humans stills being a matter of concern to structural engineers due to recurrent cases of excessive vibration in pedestrian structures (Sanderson [1], Tilly [2]). This is an indication that current design standards are incapable of effectively predicting the dynamic response of structures under the effect of human loads. The harmonic force model has been traditionally adopted to assess the vibration serviceability of pedestrian structures (Bachmann and Ammann [3]). However, this model does not consider the biodynamic parameters of the pedestrian, nor does it consider the influence of structural vibrations on pedestrian gait, which are key aspects when HSI occurs. Thus, several authors have adopted biomechanical models to represent the pedestrian and take these aspects into account (Da Silva, F., Pimentel [4], Shahabpoor et al. [5], Muhammad, Zandy O. ,Reynolds [6]).

Bipedal models (BMs) from biomechanics have been adopted recently by some authors for application in civil engineering [7–9]. These have been demonstrated to be more effective for describing the patterns of human locomotion (Whittington and Thelen [10], Suzuki and Geyer [11]). For example, the two phases of the gait cycle can be reproduced and the GRFs can be obtained directly by using these models. In particular, BMs with springs and dampers added on each leg have displayed a good capability to achieve GRF profiles similar to those of humans (Kim and Park [12], Li et al. [13]).

The increasing trend of adopting damped bipedal models to simulate walking pedestrians has motivated further investigation. The proposed analytical models are highly realistic. However, they lack experimental verification, even on rigid ground. In order to fill this gap, the aim of this study is to propose a set of parameters that allows the bipedal model to achieve GRFs as close as to the real ones as possible. The parameters combinations that achieved the best fit between model predictions and experimentally measured data are identified through multiple simulations. Based on these results empirical values for pendulum length, attack angle, leg stiffness and leg damping are proposed.

2 Methodology

2.1 Bipedal walking model

A bipedal model based on Qin et al. [7] model was adopted to represent a walking pedestrian. The lumped mass on top is supported by two straight, massless legs with springs and dampers modeled in parallel (Fig. 1). The pedestrian motion is given by the longitudinal and vertical displacements of the CM and are expressed in Cartesian coordinates (x_{cm}, z_{cm}). The legs are considered to display identical properties and the foot is represented by a point, disregarding the trajectory of the center-of-pressure during stance.

The gait cycle is defined as the interval between successive heel impacts of a foot and is divided into two phases: the single support phase (SS) and double support phase (DS). A gait cycle performed by the bipedal model is shown in Fig. 1. The model begins at the heel impact, which is defined mathematically by the condition $z_{cm} = L_p \sin\theta_{in}$. Here, θ_{in} defines the orientation of the leg in relation to the contact surface when DS is initiated. The pendulum length L_p is the maximum length of the legs owing to the stretching of the springs. The transition from DS to SS occurs when the trailing leg attains the length L_p and leaves the ground. Thus, this leg swings until the initial condition is attained, wherein it is repositioned in front of the CM. This completes the gait cycle, and the leg becomes the leading leg for the next cycle.

The leg stiffness and leg damping are constant during walking and are represented by k_l and c_l, respectively. However, the effective stiffness and damping are modeled as time-variant, and expressed as functions of k_l and c_l, as can be seen in Eq.(1). During DS the damping of the leading leg varies from zero at the beginning of contact of the leading leg to c_l at the end of contact of the trailing leg.

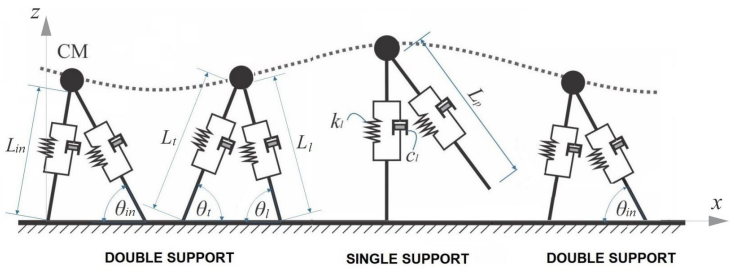

Figure 1. Scheme of bipedal model used to model a walking human, representing a gait cycle [7].

The mass, stiffness, and damping matrices of the human body were obtained by applying Newton formulation. From the force balance, the pedestrian movement is described by

$$\begin{bmatrix} m_h & 0 \\ 0 & m_h \end{bmatrix} \begin{bmatrix} \ddot{z}_{cm} \\ \ddot{x}_{cm} \end{bmatrix} + \begin{bmatrix} c_{1,1} & c_{1,2} \\ c_{2,1} & c_{2,2} \end{bmatrix} \begin{bmatrix} \dot{z}_{cm} \\ \dot{x}_{cm} \end{bmatrix} + \begin{bmatrix} k_{l,z} + k_{t,z} & 0 \\ 0 & k_{l,x} - k_{t,x} \end{bmatrix} \begin{bmatrix} z_{cm} \\ x_{cm} \end{bmatrix} = \begin{bmatrix} -m_h g \\ 0 \end{bmatrix} \tag{1}$$

where

$$\begin{aligned}
c_{1,1}(t) &= \alpha(t) c_l \sin^2\theta_l(t) + (1-\alpha(t))\, c_l \sin^2\theta_t(t) \\
c_{1,2}(t) &= c_{2,1} = -\alpha(t) c_l \sin\theta_l(t)\cos\theta_l(t) + (1-\alpha(t))\, c_l \sin\theta_t(t)\cos\theta_t(t) \\
c_{2,2}(t) &= \alpha(t) c_l \cos^2\theta_l(t) + (1-\alpha(t))\, c_l \cos^2\theta_t(t) \\
\alpha(t) &= \left(\tfrac{L_t(t)-L_{in}}{L_p-L_{in}}\right)
\end{aligned}$$

$$\begin{aligned}
k_{l,z}(t) &= k_l\left(1-\tfrac{L_p}{L_l(t)}\right) \quad k_{t,z}(t) = k_l\left(1-\tfrac{L_p}{L_t(t)}\right) \\
k_{l,x}(t) &= \left(1-\tfrac{L_p}{L_l(t)}\right)\left(\tfrac{n_s d_s}{x_{cm}(t)}-1\right) \quad k_{t,x}(t) = \left(1-\tfrac{L_p}{L_t(t)}\right)\left(1-\tfrac{(n_s-1)d_s}{x_{cm}(t)}\right)
\end{aligned}$$

$$L_l(t) = \sqrt{\left(n_s d_s - x_{cm}(t)\right)^2 + z_{cm}(t)^2} \quad L_t(t) = \sqrt{\left(x_{cm}(t) - (n_s-1)d_s\right)^2 + z_{cm}(t)^2}$$

In all the above terms, the subscripts l, t correspond to the leading and trailing legs, respectively, and x, z correspond to longitudinal and vertical directions, respectively. m_h is the mass of the body; c and k are the damping and stiffness, respectively, acting in each direction; d_s is the step length; n_s is the step number; $m_h g$ is the gravitational force acting at the body's CM; and $\ddot{z}_{cm}$, $\ddot{x}_{cm}$ and $\dot{z}_{cm}$, $\dot{x}_{cm}$ are the acceleration and velocity, respectively, of the CM in each direction. The terms L_l, L_t and θ_l, θ_t are the length and orientation of the legs at a specified time, and L_{in} is the length of the trailing leg at the beginning of DS, as shown in Fig. 1.

The GRF in the vertical direction for the leading and trailing legs, respectively, is determined by

$$\begin{aligned} GRF_l(t) &= (F_{s,l}(t) + F_{d,l}(t)) \sin\theta_l(t) \\ GRF_t(t) &= (F_{s,t}(t) + F_{d,t}(t)) \sin\theta_t(t) \end{aligned} \tag{2}$$

where $F_{s,1}, F_{s,2}$ and $F_{d,1}, F_{d,2}$ are the elastic and damping forces, respectively, acting on the legs. These are given by

$$\begin{aligned} F_{s,l}(t) &= k_l \left(L_l(t) - L_p\right) \\ F_{s,t}(t) &= k_l \left(L_t(t) - L_p\right) \end{aligned} \tag{3}$$

$$\begin{aligned} F_{d,l}(t) &= \alpha(t) c_l(-\dot{x}_{cm}(t)\cos\theta_l(t) + \dot{z}_{cm}(t)\sin\theta_l(t)) \\ F_{d,t}(t) &= (1-\alpha(t))\, c_l(-\dot{x}_{cm}(t)\cos\theta_t(t) + \dot{z}_{cm}(t)\sin\theta_t(t)) \end{aligned} \tag{4}$$

It should be noted that damping and stiffness matrices in Eq.(1) are time-variant. Also, the formulations are based on the DS phase. Thus, when the pedestrian is in the SS phase, the parts of the coefficients related to the swinging leg must be equated to zeros in Eqs.(1) to (4), and the coefficient $\alpha(t)$ must be equated to one.

Although the equations of motion are presented for horizontal and vertical directions, an approach similar to that of Gao et al. [9] is adopted in this study. For practicality, the horizontal motion is imposed by adopting a fixed horizontal speed $\dot{x}_{cm}$. Thus, the model is reduced to a single degree of freedom system, self-exciting in vertical direction.

Finally, the pedestrian movement and the GRF over time are determined by applying the Runge–Kutta fourth order integration method to solve the nonlinear equation of motion in the vertical direction from Eq.(1).

2.2 Experimental program

A series of experimental tests were conducted at the Structures Laboratory of the Alberto Luiz Coimbra Institute for Graduate Studies and Research in Engineering at the Federal University of Rio de Janeiro (LabEst-COPPE/UFRJ). The tests were designed to measure the GRFs produced by walking humans on walks on a rigid surface. To this end, bespoke force plates with dimensions of 0.90 $\times$ 0.90 m were used to measure the forces generated by walking pedestrians during the tests. A slab completely covered by force plates of this type was placed directly over the ground. This caused the surface to be rigid.

Forty-five volunteers were recruited to participate in the tests, of which 51 $\%$ were female. These proportions approximate the Brazilian population highly reasonably. Other parameters such as the height, leg length (considering the hip joint as a reference) and height to the CM (considering the navel as a reference level) were measured. The pedestrian parameters are summarized in Table 1.

The participants were asked to walk over the force plates at three speeds: slow, normal, and fast. The pedestrians' natural walking pace was considered, i.e., no restrictions were imposed to control their pacing rate. Thus, the gait speed was established according to the pedestrian's criterion. Each volunteer made a round trip three times at each walking speed along a row of aligned force plates. In total, one hundred and thirty five tests were performed.

Six adjacent force plates in the middle of the path recorded the GRFs during the tests. As the pedestrians tend to accelerate at the beginning and decelerate close to the end of the path, the walking forces were recorded halfway to ensure that the walking speed was as constant as possible. In addition, the vertical acceleration approximately at the pedestrian's CM was measured by a resistive accelerometer (Kyowa Ltd model ASW1A, capacity of 9.8 m/s^2) fixed on an acrylic plate that was fastened firmly to a belt around each pedestrian's waist. The belt was specially

Table 1. Summary of pedestrian parameters

	Age(years)	m_h(kg)	h(m)	L_{leg}(m)	h_{cm}(m)
Mean	29.7	68.5	1.70	0.89	1.03
Max	58.0	108	1.88	1.00	1.13
Min	21.0	39.8	1.48	0.73	0.86
Std	7.01	13.8	0.08	0.06	0.06

m_h: body mass; h: height; L_{leg}: leg length; h_{cm}: center-of-mass height

built for this purpose, with the aim of keeping the accelerometer as vertical as possible. The small rotations during walking due to tilting and propelling of the body were neglected.

The force and acceleration signals were recorded simultaneously, using the same Data Acquisition (DAQ) System, with a sampling frequency of 100 Hz and filtered with a 25 Hz low-pass filter. The pedestrians' path and test setup are shown in Fig. 2.

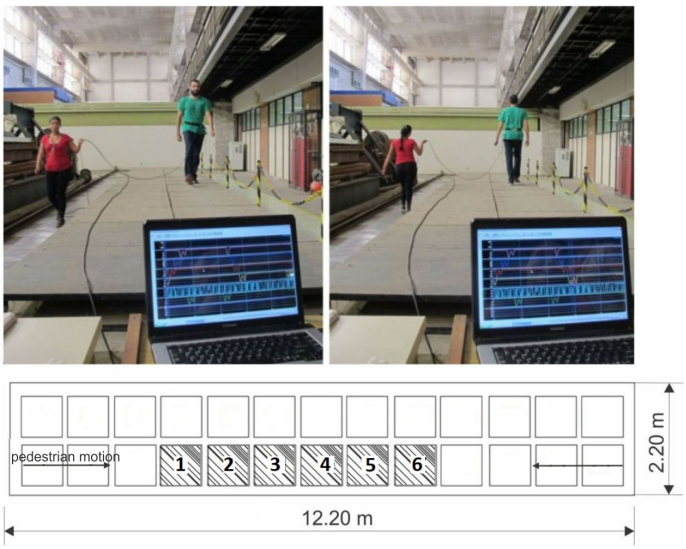

Figure 2. Typical pedestrian path during the tests. The force plates used are represented hatched in the layout.

2.3 Pedestrian data measured experimentally

The overall walking speed for each trial was estimated from the initial and final times recorded by the force plates and the distance traveled by the pedestrian. The overall pacing rate was obtained from the spectrum of accelerations measured at the pedestrian's CM. The average step length was obtained as the ratio of the average walking speed to the average pacing rate. Table 2 shows the overall walking speed, pacing rate, and step length for all the trials with slow, normal, and fast speeds.

Table 2. Summary of average pacing rate, walking speed, and step length during the tests

Trials	f_s(Hz)	v_s(m s^{-1})	d_s(m)
Slow	1.61±0.16	0.92±0.10	0.56±0.05
Normal	1.81±0.13	1.16±0.12	0.64±0.05
Fast	2.08±0.13	1.54±0.14	0.76±0.08

f_s: average pacing rate; v_s: average walking speed; d_s: average step length

The GRF was considered as the representative feature of the human gait in this study, therefore this parameter was selected to be fitted to experimental measurements. As in Whittington and Thelen [10] and Kim and Park

[12], all the one-step GRF curves were extracted from each test and averaged to reproduce an average GRF. Then, it was selected the GRF curve with less noise and minimum difference with respect to the average GRF to be representative of each pedestrian for each of the walking speeds. These representative GRFs were used for comparison with the model predictions.

2.4 Estimation of model parameters

Each combination of mass m_h, pendulum length L_p, step length d_s, leg stiffness k_l and leg damping ratio ξ_l produces a different GRF profile and specific initial conditions, which are given by initial orientation of the leg θ_{in} and initial vertical velocity $\dot{z}_{cm}(0)$. The numerical integration algorithm converges to stable gait as long as the parameters are well selected and the initial conditions are established within a certain tolerance.

Model solutions were generated multiple times (10,000 simulations for each correlation case) over a range of random parameters and initial conditions. The pedestrian mass was fixed, whereas the remaining parameters were randomly generated from uniform distributions within specified ranges. For the walking speed and pacing rate were accepted values within one standard deviation of the experimentally measured values, as in Whittington and Thelen [10]. The pendulum length has been reported by Dang [14] and Li et al. [13] to be around 20 $\%$ larger than the actual leg length (i.e. $L_p \approx 1.2L_{leg}$). Thus, the search range was set from L_{leg} to $1.3L_{leg}$. The leg stiffness was considered in the range of 10 kNm^{-1} to 40 kNm^{-1}, the leg damping in the range of 0 to 15 $\%$, and the initial orientation of the leg in the range of 62^0 to 78^0. These values were adopted based on values previously reported by Kim and Park [12], Dang [14] and Li et al. [13].

For each simulation, the Mean Relative Error (MRE) between measured and simulated GRF was computed as a measure of goodness of fit. After completing each set of 10,000 simulations, the MREs were sorted in the ascending order and the model solutions that produced the minimum MRE were selected as best matches. Then, the parameters' combinations that produced the minimum error were selected and averaged to produce a representative set of parameters for the pedestrian for the simulated walking speed.

3 Results and discussion

The procedure described in the previous section was used to match the model predictions with the representative GRFs measured experimentally and thus, obtain sets of parameters for the model to represent each of the pedestrians at different walking speeds.

An example of the result of the correlation between the model prediction and the experimental GRF, achieved for a test subject at three walking speeds, is shown in Fig. 3. The MREs between these numerical and experimentally measured profiles are 7 $\%$ for slow walking, 12 $\%$ for normal walking, and 20 $\%$ for fast walking. It is verified that the parameters obtained allow the model to approximately reproduce the variation in GRF's peak amplitudes and stance time according to the walking speed (Fig. 3a,c,e). In addition, the correlation with the experimental measurements in time domain is better at lower gait speeds than at higher gait speeds. The higher the gait speed, the higher is the amplitude of the first peak, which tends to overestimate the vertical GRF's amplitudes. Furthermore, the typical M-shape becomes sharper, thereby achieving lower values around mid-stance, as can be seen in Fig.3e. These results are in agreement with those of Kim and Park [12], in which it was reported better performance of the model at slow at normal walking speeds. This effect can be explained by the fact that the foot's geometry is disregarded in this model. It was demonstrated by Whittington and Thelen [10] that the introduction of a roller foot in the bipedal spring–mass model decreases the magnitude of the vertical peaks, and the GRF tends to flatten around mid-stance.

In Fig. 3b,d,f it is shown the comparison in the frequency domain. In these examples, the pacing rate of the model matched the pacing rate measured experimentally. It is worth mentioning that the experimental spectrums have been obtained by reconstructing the GRF-time history from the representative experimental GRF for comparison. This is justified because the simulations were carried out considering identical parameters and initial conditions for each step, whereas the actual gait is not perfectly periodic. It can be seen, the higher the walking speed, the higher is the fundamental harmonic amplitude. This is intuitive because the walking pattern is closer to that of running at higher speeds, which results in higher accelerations in the vertical direction. The numerical results show that the model has the capability to reproduce that pattern and thereby, describe the kinematics of the human body consistently. The best agreement between the harmonics' amplitudes is found for normal walking. The comparison of accelerations at the pedestrian's CM at three walking speeds is shown in Fig.4.

The gait speeds of the fitted tests are in the range 0.82–1.56 m s^{-1}. The model was not capable of reproducing the GRF effectively for gait speeds outside this range. When a pedestrian walks at too low speeds, the GRF profile

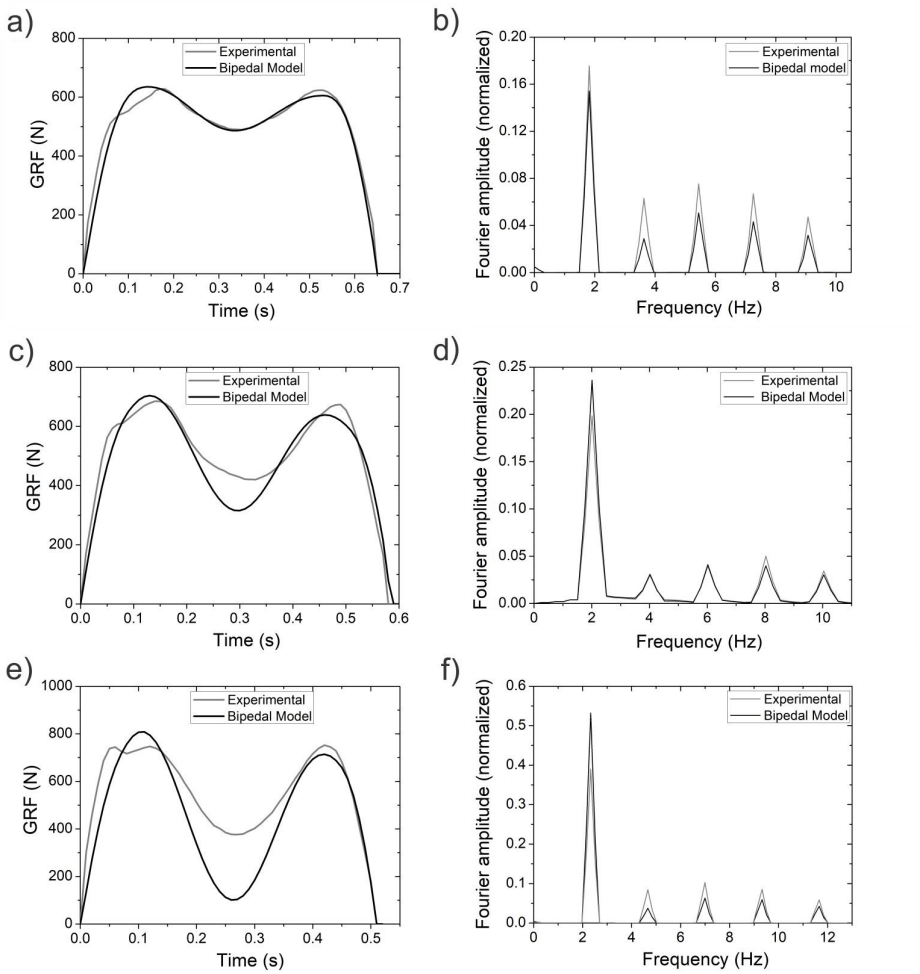

Figure 3. Comparison between model predictions (dark lines) and experimental measurements (grey lines) of GRF in time and frequency domains: a) slow walking; b) normal walking and c) fast walking.

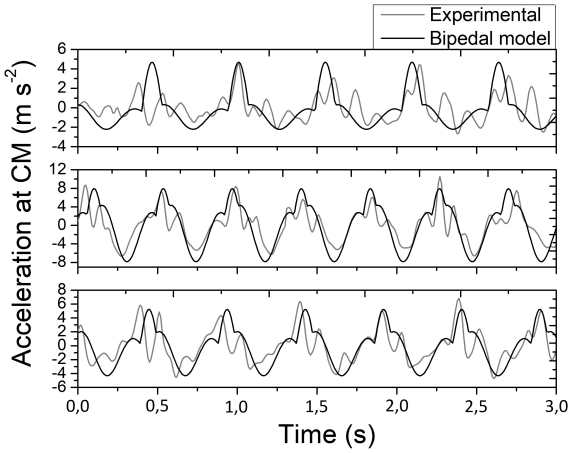

Figure 4. Typical comparison between model predictions (dark lines) and experimental measurements (grey lines) of accelerations at pedestrian's CM: a) slow walking; b) normal walking and c) fast walking.

tends to appear with only one peak around mid-stance. In contrast, when the gait speed is too high, the GRF profile tends to be so deep around mid-stance that it assumes negative values. Modeling the roller foot could improve the model performance at higher speeds. However, the model in question is suitable to reproduce normal walking speed.

In total, 89 experimental tests were adjusted by the bipedal model out of 135 performed, 27 at slow walking,

38 at normal walking and 24 at fast walking. It means, it was obtained 89 sets of parameters that represent several pedestrians at different walking speeds.

4 Closing remarks

This paper presents the results of validation of a bipedal walking model with respect to extensive experimental measurements from tests involving walking humans. The bipedal model parameters were identified by correlating the predicted and measured GRFs. The model produced GRFs profiles that reassemble the experimental measurements in the speed range of 0.82–1.56 ms^{-1}. These values correspond to the pacing frequency in the range of 1.42-2.42 Hz. The pendulum length of the model was found to be in the range of 0.98-1.26 m, the initial orientation of the leg in the range of 68-74°, the leg stiffness in the range of 13-34 kNm^{-1} and the leg damping ratio in the range of 3-13 $\%$. The bipedal model performed better at slow and normal walking speeds. The predicted and measured GRFs were quite proximate at these speeds. Otherwise, at faster speeds, the numerical GRF presented larger deviations from the experimental measurements at the central part of the curve. The accelerations simulated at the pedestrian center of mass were also consistent with the experimental measurements, demonstrating the model capability to properly simulate the locomotion of the human body. Overall, the results of this study suggest that the parameters obtained for the bipedal model are useful to simulate walking pedestrians at slow and normal walking speeds. However, there is a need for further calibrations with respect to experimental observations to provide a more reliable database.

Acknowledgements. This research was also supported by the Brazilian National Council for Scientific and Technological Development (CNPq) under Grant (141844/2016-7).

Authorship statement. The authors hereby confirm that they are the sole liable persons responsible for the authorship of this work, and that all material that has been herein included as part of the present paper is either the property (and authorship) of the authors, or has the permission of the owners to be included here.

References

[1] K. Sanderson. Millennium Bridge wobble explained. *Nature*, 2008.
[2] G. P. Tilly. Dynamic behaviour and collapses of early suspension bridges. *Proceeding of the Institution of Civil Engineers - Bride Engineering*, vol. 164, n. 2, pp. 75–80, 2011.
[3] H. Bachmann and W. Ammann. Vibrations in structures: induced by man and machines. *International Associatiom for Bridges and Structural Engineering*, 1987.
[4] R. Da Silva, F., Pimentel. Biodynamic walking model for vibration serviceability of footbridges in vertical direction. In *Proceedings of the 8th International Conference on Structural Dynamics*, pp. 1090–1096, Leuven, 2011.
[5] E. Shahabpoor, A. Pavic, V. Racic, and S. Zivanovic. Effect of group walking traffic on dynamic properties of pedestrian structures. *Journal of Sound and Vibration*, vol. 387, pp. 207–225, 2017.
[6] P. Muhammad, Zandy O. ,Reynolds. Probabilistic Multiple Pedestrian Walking Force Model including Pedestrian Inter- and Intrasubject Variabilities. *Advances in Civil Engineering*, vol. 2020, pp. 1687–8086, 2020.
[7] J. W. Qin, Q. S. Yang, and S. S. Law. Pedestrian–bridge dynamic interaction, including human participation. *Journal of Sound and Vibration*, vol. 332, n. 4, pp. 1107–1124, 2013a.
[8] J. W. Qin, S. S. Law, Q. S. Yang, and N. Yang. Finite Element Analysis of Pedestrian-Bridge Dynamic Interaction. *Journal of Applied Mechanics*, vol. 81, n. 04, pp. 41001, 2013b.
[9] Y.-A. Gao, Q.-S. Yang, and J.-W. Qin. Bipedal Crowd–Structure Interaction Including Social Force Effects. *International journal of structural stability and dynamics*, vol. 17, n. 07, pp. 1750079, 2017.
[10] B. R. Whittington and D. G. Thelen. A Simple Mass-Spring Model With Roller Feet Can Induce the Ground Reactions Observed in Human Walking. *Journal of biomechanical engineering*, vol. 131, n. 1, 2009.
[11] Y. Suzuki and H. Geyer. A simple bipedal model for studying control of gait termination. *Bioinspiration & Biomimetics*, vol. 13, n. 3, pp. 36005, 2018.
[12] S. Kim and S. Park. Leg stiffness increases with speed to modulate gait frequency and propulsion energy. *Journal of biomechanics*, vol. 44, n. 7, pp. 1253–1258, 2011.
[13] T. Li, Q. Li, and T. Liu. An actuated dissipative spring-mass walking model: Predicting human-like ground reaction forces and the effects of model parameters. *Journal of biomechanics*, vol. 90, pp. 58–64, 2019.
[14] H. V. Dang. *Experimental and Numerical Modelling of Walking Locomotion on Vertically Vibrating Low-Frequency Structures*. PhD thesis, University of Warwick, 2014.